First record of Cricetops rodent in the Oligocene of southwestern China

Lüzhou Li, Xijun Ni, Xiaoyu Lu & Qiang Li

Taylor & Francis
Taylor & Francis Group

First record of *Cricetops* rodent in the Oligocene of southwestern China

Lüzhou Li[a] (ID), Xijun Ni[a,b] (ID), Xiaoyu Lu[a] (ID) and Qiang Li[a,b] (ID)

[a]Key Laboratory of Vertebrate Evolution and Human Origins, Institute of Vertebrate Paleontology and Paleoanthropology, Chinese Academy of Sciences, Beijing 100044, China; [b]Chinese Academy of Sciences –CAS Center for Excellence in Tibetan Plateau Earth Sciences, Beijing 100101, China

ABSTRACT

The muroid *Cricetops* Matthew and Granger, 1923 commonly occurred in the Oligocene terrestrial deposits in central and northern Asia. Here we report the first record of *Cricetops* in the southern part of Asia. Isolated rodent molars named as a new species, *Cricetops auster* sp. nov., were discovered from the early Oligocene sediments at the Lijiawa locality in Yunnan Province in southwestern China. Compared to previously known *Cricetops*, *C. auster* is smaller than *Cricetops dormitor* Matthew and Granger, 1923 and *Cricetops aeneus* Shevyreva, 1965, but larger than *Cricetops minor* Wang, 1987. The cusps of *C. auster* are less conical. The ridges and crests are longer, higher and thicker. Relatively long and high crests, ridges and arms extending from the main cusps in the new species make those cusps more crescent in appearance than in *C. dormitor*, *C. aeneus* and *C. minor*. *C. auster* is a rare species in the Lijiawa mammalian fauna. Well-developed shearing tooth crests and ridges of *C. auster* probably suggest a different diet from the *Cricetops* from the northern part of Asia.

Introduction

Cricetops Matthew & Granger, 1923 rodents occurred in a wide area of Oligocene deposits in Mongolia, Kazakhstan and many localities in northern China (Figure 1). Literally, *Cricetops* means a hamster-like rodent. Morphologically, however, it is an enigmatic rodent: it has cricetid dental morphology but hystricomorphous zygoma (Matthew & Granger 1923; Carrasco & Wahlert 1999). Compared with the contemporaneous cricetids, such as *Eucricetodon* Thaler, 1966 and *Paracricetops* Maridet and Ni, 2013, *Cricetops* appears to be much more 'derived' by its enormously large size, twinned anterocones and strange crenulation of the dental enamel. *Cricetops* is usually a dominant element in the early Oligocene faunas in North and Central Asia. For instance, the specimens of *Cricetops dominor* Matthew and Granger, 1923 alone account for more than one-third of all the roughly 3300 mammalian specimens collected from the Hsanda Gol Formation of Mongolia during the American Museum of Natural History Central Asiatic Expedition (Mellett 1968). *Cricetops* is therefore widely regarded as an 'index taxon' of the Early Oligocene in Asia (Matthew & Granger 1923; Argyropulo 1938; Shevyreva 1967; Kowalski 1974; Ni et al. 2007; Russell & Zhai 1987; Wang 1987). In South and Southeast Asia, however, *Cricetops* was not known previously. Here we report a new species of *Cricetops* discovered from the earliest Oligocene of Yunnan Province in Southwest China. The discovery suggests that *Cricetops* were indeed present in the early Oligocene tropic and subtropic region of Asia. As relatively, a rare member of the mammalian fauna from the early Oligocene of Yunnan, the new

species of *Cricetops* was probably adapted to a different environment from their relatives living in the northern part of Asia.

Geological background

The *Cricetops* fossil reported here was discovered from a fossil locality near the Lijiawa Village of Qujing County. The locality lies about 125 km northeast of Kunming (capital of Yunnan Province) and 20 km southeast of Qujing City. The Paleogene deposits at the Lijiawa fossil locality include two rock units, the Caijiachong Formation and the unconformably underlying Gelanghe Formation. The Caijiachong Formation is a set of grayish-green silty mudstone and grayish-green mudstone. The Gelanghe Formation consists of a set of thick reddish-brown maroon mudstone and siltstone with gravels and calcareous concretion, and a set of poorly graded breccias cemented by sandy marl. More than 40 taxa have been collected from the lower part the Caijiachong formation. These taxa constituted the Caijiachong Mammalian Fauna. The age of this fauna is Ulangochuan or Late Ergilian (Naduan + Ulangochuan) of the Asian Land Mammalian Age, which has been correlated with the North American Chadronian or European MP19 (Wang 1985, 1992, 1997a, 1997b; Emry et al. 1998; Wang 2001; Maridet & Ni 2013).

The new *Cricetops* specimens reported here were collected from the uppermost fossiliferous layer of the Caijiachong Formation. More than 10 mammalian taxa had been collected in this layer, including the new species of *Cricetops* and the recent named pen-tailed tree shrew *Ptilocercus kylin* Li and Ni, 2016.

Figure 1. Distribution of *Cricetops*. (1) Lijiawa locality, Yunnan, China; upper Caijiachong Formation, Earliest Oligocene; *C. auster* sp. nov. nov. (2) Wulanbulage locality, Inner Mongolia, China; Wulanbulage Formation, Middle Oligocene; *C. dormitor*. (3) Sanshenggong (Saint-Jacques) locality, Inner Mongolia, China; Wulanbulage Formation, early Oligocene; *C. dormitor* and *C. minor*. (4) XJ99031 Locality, Xinjiang, China; Keziletuogayi Formation, earliest Oligocene; *C. dormitor*. (5) Hsanda Gol locality, Obor-Khangay, Mongolia; Hsanda Gol Formation, early Oligocene; *C. dormitor* and *C. aeneus*. (6) Ikh-Argalantu-Nuru locality, Obor-Khangay, Mongolia; Hsanda Gol Formation, early Oligocene; *C. dormitor*. (7) Ulan-Khureh locality, Omono Gobi, Mongolia; Hsanda Gol Formation, early Oligocene; *C. dormitor*. (8) Menkhen-Teg Locality, Obor-Khangay, Mongolia; Hsanda Gol Formation, early Oligocene; *C. dormitor*. (9) Tsakhir location, Omono Gobi, Mongolia; early Oligocene; *C. dormitor*. (10) Shunkht Locality, Omono Gobi, Mongolia; Hsanda Gol Formation, early Oligocene; *C. dormitor*. (11) Khatan-Khayrkhan locality, Gobi Altay, Mongolia; early Oligocene; *C. dormitor*. (12) Chelkar-Teniz locality, Aktyubinsk Oblast, Kazakhstan; Chilikty Formation, early Oligocene; *C. dormitor* and *C. aeneus*. (13) Sary-Su locality, Chimkent Oblast, Kazakhstan; Betpakdaka Formation, early Oligocene; *C. dormitor*. (14) Kyzyl-Kak locality, Dzhezkazgan Oblast, Kazakhstan; Betpakdaka Formation, early Oligocene; *C. dormitor*. (15) IM0513 locality, Sonid Zuoqi, Inner Mongolia, China, early Oligocene; *C. dormitor* and *C. minor*. (16) K15 locality, Zaysan Basin, Kazakstan; Buran Svita, early Oligocene; *C.* sp. (17) Ulariya locality, Olkhon Island, Baikalian Region, Russia; early Oligocene; *C.* cf. *dormitor*. Distribution of *Cricetops* is based on the data in references (Wang et al. 1981; Russell & Zhai 1987; Wang 1987; Emry et al. 1998; Ni et al. 2007; Erbajeva & Alexeeva 2013).

Notes: The background map is modified from https://commons.wikimedia.org/wiki/File:World_map_(Miller_cylindrical_projection,_blank).svg (under the Creative Commons Share Alike license: https://creativecommons.org/licenses/by-sa/3.0/deed.en).

These fossils show more derived features than those from the Caijiachong Fauna, and clearly indicate an early Oligocene age for the Lijiawa Mammalian Fauna (Maridet & Ni 2013; Li & Ni 2016). For instance, the amynodontid (Perissodactyla) specimens identified as *Gigantamynodon* cf. *giganteus* Xu, 1961 is about 20% larger than the late Eocene *G. giganteus* from the Caijiachong fauna. The specimens identified as *Eucricetodon caducus* Shevyreva, 1967 are closely similar to those discovered from the earliest Oligocene of Xinjiang, China and Hsanda Gol, Mongolia (Ni et al. 2007; Maridet & Ni 2013). Those specimens are much more derived than the *Eucricetodon* and *Eocricetodon* species from the late Eocene Caijiachong fauna by their larger size, broader anterocone in M1 and better developed anteroconid in m1.

Materials and methods

The *Cricetops* specimens are publicly deposited and accessible in the collections of the Institute of Vertebrate Paleontology and Paleoanthropology, Chinese Academy of Sciences (142 Xi Zhi Men Wai Street, Beijing, China). All the specimens were discovered during the field expeditions supported by the Chinese Academy of Sciences, the Ministry of Science and Technology of China, and the National Natural Science Foundation of China. No permits were required for this study, which complied with all relevant regulations.

The specimens reported here were collected via screen-washing at the Lijiawa locality. More than 100 tons of matrix were processed. Totally 12 isolated teeth were identified as a new species of *Cricetops* and reported here. After cleaning, the specimens were CT-scanned using the 225 kv Micro-CT at the Key Laboratory of Vertebrate Evolution and Human Origins, Chinese Academy of Sciences. Segmentation and 3D virtual reconstruction were done by following the standard procedure introduced by Ni et al. (2012). Specimens were measured using Zeiss SteREO Discovery V.20 stereoscopic microscope with a precision of 0.01 mm. The tooth morphological and orientation terminology follows that of Maridet and Ni (2013).

Results

Systematic paleontology
Rodentia Bowdich 1821
Muroidea Illiger 1811
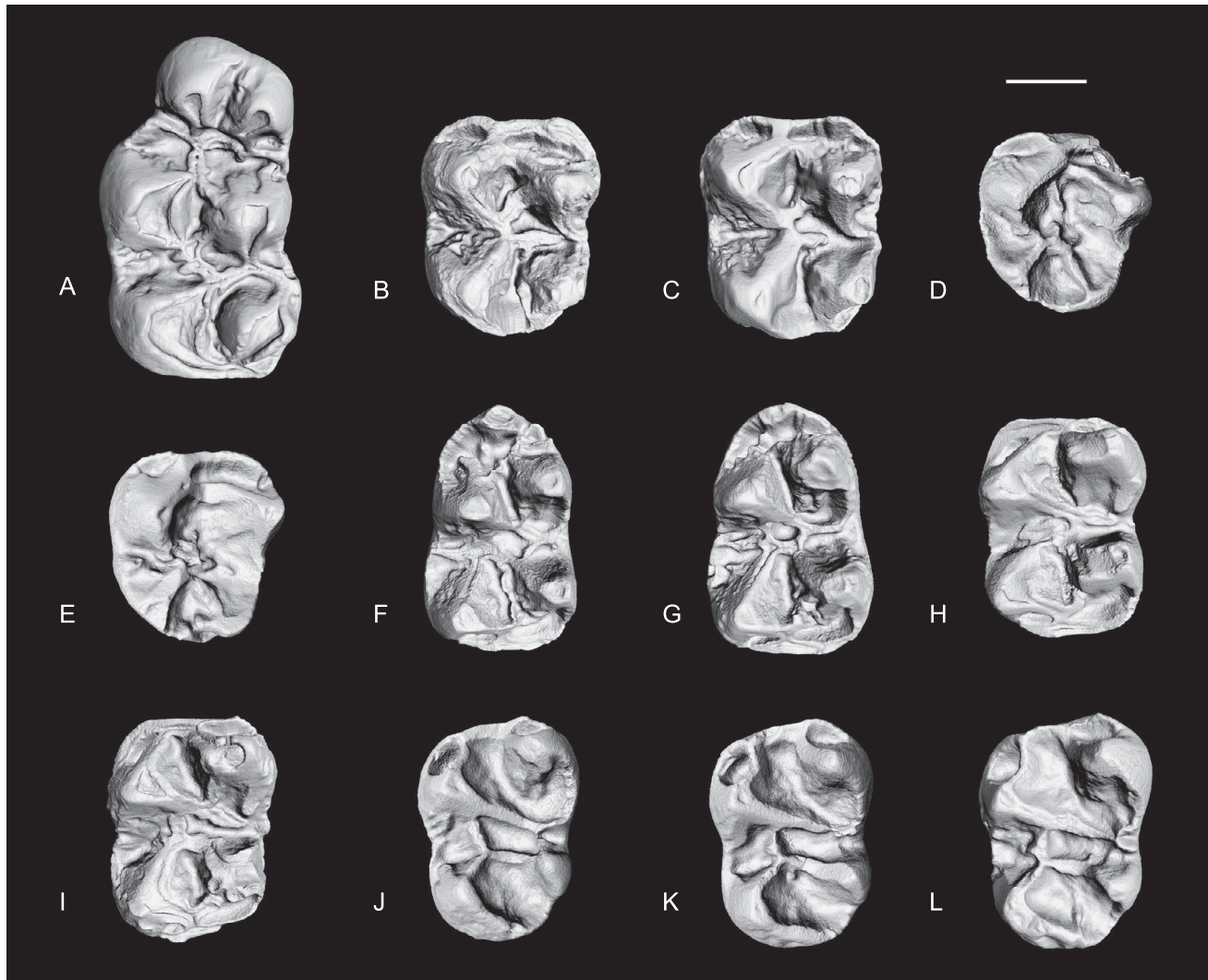Cricetidae Fischer von Waldheim 1817

Figure 2. Dentition of *Cricetops auster* sp. nov. (A) left M1 (V 22635, holotype); (B) left M2 (V 22636.1); (C) left M2 (V 22636.2); (D) right M3 (V 22636.3, reversed); (E) right M3 (V 22636.4, reversed); (F) left m1 (V 22,636.5); (G) left m1 (V 22636.6); (H) left m2 (V 22636.7); (I) left m2 (V 22636.8); (J) right m3 (V 22636.9, reversed); (K) right m3 (V 22636.10, reversed); (L) left m3 (V 22636.11).
Note: Scale bar, 1 mm.

Table 1. Measurements for *Cricetops auster* sp. nov.

Specimen number	Tooth loci	Side	Length (mm)	Width (mm)
IVPP V22635	M1	Left	4.27	2.42
IVPP V22636.1	M2	Left	2.90	2.28
IVPP V22636.2	M2	Left	2.74	2.29
IVPP V22636.3	M3	Right	2.22	2.15
IVPP V22636.4	M3	Right	2.17	2.21
IVPP V22636.5	m1	Left	3.26	1.94
IVPP V22636.6	m1	Left	3.08	2.09
IVPP V22636.7	m2	Left	2.93	2.13
IVPP V22636.8	m2	Left	2.85	2.16
IVPP V22636.9	m3	Right	2.93	2.06
IVPP V22636.10	m3	Right	2.85	2.07
IVPP V22636.11	m3	Left	2.96	2.20

Cricetopinae Matthew and Granger, 1923
Cricetops Matthew and Granger, 1923
Cricetops auster sp. nov. (Figure 2; Table 1)

Type specimen

IVPP V 22635, a left M1.

Referred specimens

Left M2, IVPP V 22636.1; left M2, IVPP V 22636.2; right M3, IVPP V 22636.3; right M3, IVPP V 22636.4; left m1, IVPP V 22636.5; left m1, IVPP V 22636.6; left m2, IVPP V 22636.7; left m2, IVPP V 22636.8; right m3, IVPP V 22636.9; right m3, IVPP V 22636.10; left m3, IVPP V 22636.11.

Locality and age

Near Lijiawa Village, southeast to Qujing City, Yunnan, China. Upper Caijiachong Formation, Early Oligocene.

Diagnosis

Larger than *Cricetops minor* Wang, 1987 but smaller than *Cricetops dormitor* Matthew and Granger, 1923 and *Cricetops aeneus* Shevyreva, 1965. M1 anterocone pair significantly narrower than protocone-paracone pair and hypocone-metacone pair, proportionally similar to *C. minor*, but narrower than in *C.*

dormitor and *C. aeneus*. M1–2 valley between protocone-paracone and hypocone-metacone wider and deeper than in *C. dormitor* and *C. aeneus*. M2 metacone mesiolingual side present straight ridge. M3 metacone crest-like and much weaker than in *C. dormitor* and *C. aeneus*; mesosinus broader than in *C. dormitor* and *C. aeneus*. m1 present a deep fossa enclosed by protoconid distal arm, mesolophid and ectolophid. m3 mesial border oblique; protoconid and metaconid enclose a wide U-shaped valley; protoconid distal arm strong and straight, extending to lingual tooth border; hypolophulid long and in parallel with protoconid distal arm; mesosinusid deep and long, lingually opened.

Etymology

Specific epithet is from auster, Latin for south wind and south, in allusion to the geographic origin of the species.

Description

From the occlusal view, the crown of M1 is kidney shaped, with a slightly concave buccal border and a strongly convex lingual border. It bears three pair of opposed cusps: two anterocones, protocone and paracone, and hypocone and metacone. The anterocone pair is narrower than the other two cusp pairs. The lingual and buccal anterocone are about the same size, well divided by a deep valley, which opens mesially, and is closed distally by a weak crista. Both lingual and buccal anterocones are distally inclined, with their wear facets more distally facing than the other two pairs. The protocone and the paracone are a pair of large cusps. The protocone is slightly bigger, but lower; the paracone is smaller but sharper. The buccal side of the protocone is steep and slightly concave. The mesial and distal protocone spurs are very short, connecting the anterolophule and entoloph, respectively. The wear facet of protocone extends to the mesial and distal protocone spurs, resulting in a slightly buccal tilting crescent depression. On the lingual side of the paracone, it develops two short but obvious ridges, usually termed as mesial protolophule (protolophule I) and distal protolophule (protolophule II). The two ridges join the protocone spurs and enclose a deep fossa between protocone and paracone. Mesially, the paracone bears a low spur, which extends mesiobuccally and joins the transverse ridge between the anterocone and paracone. Distally, the paracone bears a very strong paracone spur, which joins the mesoloph distally. The wear facet of the paracone extents to the paracone spur and forms an inverted waterdrop shape. The hypocone and metacone pair is roughly in the same form as the protocone and paracone pair. Mesiobuccally, the hypocone bears a short hypocone spur that joins the entoloph and mesoloph. Distobuccally, the hypocone is tapered and continued with the long posteroloph, which extends far buccally and defines the distal border of the tooth. Like in the protocone, the wear facet of the hypocone is crescent shaped. The metacone is quite round. Its mesiobuccal side tapers into a strong ridge, equivalent to the metacone ridge in many other cricetids. This ridge connects the mesoloph near the buccal border. Distolingually, the metacone tapers into another very short but strong ridge, which is equivalent to the metalophule. This short metalophule connects the posteroloph distally. The wear facet of metacone extends onto the metacone ridge and metalophule, and forms a lanceolate depression. The mesial hypocone spur, the mesoloph, the metacone ridge, the

metalophule, the posteroloph and the hypocone and metacone themselves enclose a deep C-shaped valley.

Between the anterocones, the protocone-paracone pair and the hypocone-metacone pair, there are two deep transverse valleys on M1. In those two valleys, the tooth crown is quite crenulated and bears many long and short ridges that divide the valleys and enclose many small fossae. Along the buccal and lingual tooth borders, respectively, the valley between the anterocone pair and the protocone-paracone pair is closed by low and incomplete buccal and lingual anterolophs. In the middle of the valley, a strong anterolophule connects the lingual anterocone and the protocone-paracone pair, therefore divides the valley into the protosinus at the lingual side and the anterosinus at the buccal side. A short lingual ridge and a long and strong buccal ridge are developed from the mesial part of the anterolophule. The two transverse ridges (lingual and buccal spurs of the anterolophule) further divide the protosinus and anterosinus into mesial and distal parts, respectively. On its distal side, the buccal anterocone bears a short spur that connects the buccal transverse ridge, further complicating the crenulation pattern.

In the valley between the protocone-paracone pair and hypocone-metacone pair, the strong and oblique entoloph of M1 divides the valley into the lingual part, termed as sinus, and the buccal part, termed as mesosinus. The sinus is deep and roughly triangular. The mesosinus is further divided by the transversely running mesoloph, the paracone spur and the metacone ridge into several fossae. The paracone spur and the buccal part of the mesoloph define a triangular fossa near the buccal border. A similar fossa is also observed in *Paracricetops*.

The M2 is much smaller than the M1, and only has two pairs of the cusps. The occlusal view of the M2 is roughly square, with the distal part slightly narrower than the mesial part. The mesial border of the tooth is defined by very strong anteroloph. The loph is transversely straight, with posteriorly bending lingual and buccal ends, which connect with the protocone and paracone, respectively. The buccal one is longer than the lingual one. A short but robust anterolophule links the anteroloph and protocone crossing the narrow but deep valley between the anteroloph and protocone-paracone pair. The protocone and the paracone, and the protolophules connecting the two cusps are arranged in the same pattern as in the M1, as well as the deep fossa enclosed between the protocone and paracone. Different from the M1, the hook-like distal paracone spur is much stronger and longer. It runs distobuccally and delimits a small pit on its mesial side. The hypocone-metacone cusp pair is also arranged in the same pattern as in M1, but the metacone is much smaller. The hypocone tapers mesiobuccally and forms a strong ridge. Distobuccally, the hypocone has a much weaker posteroloph than in M1. The metacone is buccolingually compressed and in a wedge shape. It bears a strong mesial ridge and a strong distal ridge, which is equivalent to the metalophule widely present in other cricetids. The mesial metacone ridge extends for a short distance to meet the distal end of the paracone spur near the buccal border, where a small mesostyle is formed. The metalophule connects the posteroloph and encloses a broad fossa with the latter. Buccally to the metalophule and distobuccal to the metacone, a small depression is formed near the tooth border. The mesiolingual side of the metacone bears a straight ridge.

Between the protocone-paracone and hypocone-metacone cusp pairs, the sinus and mesosinus of M2 are as deep and broad

as in those of M1. Different from the M1, the entoloph is very short, and the mesoloph does not reach the paracone spur and metacone ridge. On the distal side of the mesoloph, a small spur joins the ridge on metacone.

M3 is smaller than the M2, and roughly triangular in occlusal view. Like in M2, the buccal and lingual anterolophs define the straight mesial tooth border. The mesial protocone spur continues with the robust anterolophule, which joins the anteroloph and separates the deep protosinus and anterosinus. The cusps of the tooth have relatively smaller bases and are therefore more trenchant than those of M1 and M2, and are not arranged in obvious cusp pairs. The protocone is larger than the other cusps. It has very strong ridge-like mesial and distal spurs. The two spurs, combined with its concave and steep buccal surface, give the cusp a crescent shape. The paracone is slender, smaller and lower than the protocone. The ridges developed from the paracone include the mesial protolophule, distal protolophule and paracone spur. The mesial protolophule is a very strong oblique ridge. The distal protolophule is quite weak. The paracone spur is similarly developed as in M2. A small depression is also developed buccal to the spur. The valley between the protocone and metacone is very broad. No deep fossa as in M1 and M2 is developed. The hypocone is triangle pyramid shaped. The mesial hypocone spur is very strong, and runs mesiobuccally to join the entoloph and metalophule. The metacone is small and compressed. Its tip is located just on the tooth border and inclines distobuccally. The metalophule is as strong as the mesial spur of the hypocone. The two ridges form a big chevron. The mesial and distal ridges of the metacone define the distobuccal corner of the tooth. A deep triangle fossa is enclosed by the hypocone mesial spur, the metalophule and the distal ridge of metacone.

Proportionally, the sinus and mesosinus of M3 are much broader than in M1 and M2. Because of the weak development of the distal protolophule, the mesosinus is confluent with the valley between the protocone and the paracone, forming a very large basin and occupying about half the area of the crown. In this broad basin, several small and low ridges are developed at the position of the mesoloph.

The m1 is oval in the occlusal view, with a pointed mesial end and broad distal end, but waisted between cusps. A sharp and undivided anteroconid is mesiodistally compressed. It is mesiodistally compressed and much smaller than the other four cusps. The buccal and lingual sides of the cusp extend into high ridges, the buccal and lingual anterolophids, which define the mesial tooth edge. The two lophids have weak connection with the protoconid and metaconid. Distal to the anteroconid, the tooth bears four main cusps, arranged in two cusp pairs, protoconid-metaconid pair and hypoconid–entoconid pair. The protoconid is triangular pyramid shaped. It is bigger but lower than the metaconid, and is located more distally relative to the metaconid. The metaconid is conical with a relatively rounder base. The mesial side of the protoconid develops few low and short ridges. The strongest one can be regarded as the anterolophulid. The mesial side of the metaconid also develops a few low ridges. The strongest one can be the homologous structure of metaconid mesial spur as in other cricetid-form rodents. Mesial spurs or ridges developed from protoconid and metaconid have very low connections with the anteroconid, and low connections to close the mesial side of the valley between protoconid and metaconid. Distally, the protoconid has a long and strong distal

arm, which extends all the way to the lingual side and makes a U-turn to join the metaconid distal ridge. The metaconid distal ridge is high and thick. It develops from the tip of the metaconid and gives the cusp a 'coma' appearance. The distobuccal surface of the metaconid bears two low and short ridges. These two ridges have very weak connection with the distal arm of the protoconid. The protoconid, metaconid and ridges developed from these two cusps enclose a long U-shaped valley. This special morphology is also present in m2 and m3.

The hypoconid–entoconid pair of m1 is in a similar form as the protoconid-metaconid pair, but slightly wider with different ridge pattern. The hypoconid is triangular pyramid shaped. Its mesial side extends into the major part of the ectolophid. Its distolingual arm of the hypoconid joins the distobuccal side of the entoconid. The entoconid is roughly conical. Its mesiobuccal side extends into the short but trenchant hypolophulid. Its mesiolingual side has a faint ridge that extends to the distal arm of protoconid. Its distobuccal side has strong crenulation and forms a few small ridges to connect the distal arm of hypoconid. Its distolingual side bears a short and curved ridge, a similar structure as in metaconid. This ridge buccally merges into the posterolophid, which borders the distal edge of the tooth. The longitudinal valley between the hypoconid and entoconid is straight and deep. Both its mesial and distal sides are closed by short ridges. Distal to the hypoconid–entoconid pair, a long and slightly curved valley is defined by the two cusps and the posterolophid.

The valley between the protoconid-metaconid pair and the hypoconid–entoconid pair is broad on m1. The ridges in the valley are all quite low. No obvious mesoconid is present, but the ectomesolophid and mesolophid are present. The former is long and extends to the buccal tooth border. The latter is short. The buccal part of the mesolophid merges into the hypolophulid. The lingual part of the mesolophid joins the distal arm of protoconid. The mesolophid, ectolophid and the distal arm of protoconid enclose a small fossa.

m2 is rectangle shaped from the occlusal view, and has a waist in the middle region. The general cusp-ridge pattern is similar to that of m1. The mesial and distal ridges or arms descending from the protoconid and hypoconid are stronger than those in m1, as a result the protoconid, hypoconid and their wear facet are more crescent. The mesial tooth border bears a straight and high anterolophid. The buccal part of the anterolophid is curved and joins the protoconid distally. Mesiobuccal to the protoconid, a small but deep fossa is enclosed. The lingual end of the anterolophid is free, not joining the metaconid distally. The protoconid-metaconid pair connects the anterolophid via strong anterolophulid and metalophulid. The distal arm of protoconid and the metaconid distal ridge are not merged. A narrow gap separates the two ridges. The valley enclosed between protoconid and metaconid is curved as in m1, but it is not quite U-shaped. The hypoconid–entoconid pair and its associated ridges are very like those of m1. The most obvious difference lies in the shape of the fossa between hypoconid and entoconid. In m2, the fossa is relatively rounder and more completely enclosed.

Between the protoconid-metaconid pair and the hypoconid–entoconid pair, the transverse valley on m2 is as deep and broad as that of m1. Within the valley, the ectomesolophid and ectolophid are variably developed, and are relatively weaker

than those in m1. The mesolophid is very short and becomes a natural extension of hypolophulid. The small fossa enclosed between distal arm of protoconid and mesolophid is absent in m2.

m3 has an oval-shaped occlusal surface, with its distal part significantly narrower than its mesial side. The tooth bears four major cusps. The protoconid and metaconid are similar to those of m1 and m2, but clearly more slender. The U-shaped valley between the protoconid and metaconid is very broad. The hypoconid and entoconid are much reduced. The hypoconid is crescentic, with its mesial side descending into a short ridge and distal sider tapering as a long distal arm. The entoconid and hypolophulid merge and form a wedge-like oblique crest. This crest is parallel to the long distal arm of the protoconid. The valley between hypoconid and entoconid is very broad and becomes a distolingually open fossa. The transverse valley between the protoconid-metaconid pair and hypoconid–entoconid pair is also very broad. Within this transverse valley, a short ectolophid connects the two cusp pairs. This ectolophid is more buccally positioned than that in m1 and m2. As a result, the sinusid is shallower than in m1 and m2. In the middle of the ectolophid, a very short ectomesolophid is developed. In one m3, an obvious mesostylid is present.

Comparison

Cricetops auster sp. nov. is smaller than *Cricetops dormitor* Matthew and Granger, 1923 and *Cricetops aeneus* Shevyreva, 1965, but lager than *Cricetops minor* Wang, 1987. *C. aeneus* and *C. minor* bear stronger crests, sharper and more crescent cusps over all the molar crowns of the new species than *C. dormitory*. *C. dormitor* and *C. aeneus* are very similar to each other. The M1–2 in these two taxa has stronger mesoloph than in *C. auster*. The metacone of the M1–2 in *C. dormitor* and *C. aeneus* has a much weaker ridge on its mesiobuccal side than in *C. auster*. The mesiolingual side of the M1–2 metacone in *C. dormitor* bears a weak and blunt ridge. This ridge is similar to that in *C. auster*, but different from that in *C. aeneus*, in which this ridge is higher and joins the mesial arm of hypocone. The M3 of *C. dormitor* and *C. aeneus* has stronger metacone than that of *C. auster*. The m1 in *C. dormitor* and *C. aeneus* has bigger and more conical anteroconid than the m1 in *C. auster*. The distobuccal side of the m1 metaconid in *C. dormitor* and *C. aeneus* is smooth, and lacks the short ridge to close the valley between the protoconid and metaconid. The distal ridge of the m1 metaconid in *C. dormitor* and *C. aeneus* is weak, and it does not join the distal arm of the m1 protoconid. The valley between the distal arm of the m1 protoconid and the metaconid is very narrow, much narrower than in *C. auster*. The entoconid of *C. dormitor* and *C. aeneus* lacks a distobuccal ridge. In *C. auster*, the entoconid bears a distobuccal ridge that joins the distal arm of hypoconid and closes the valley between the hypoconid and metaconid. The m2 in *C. dormitor* and *C. aeneus* has relatively weak anterolophid. Particularly the lingual part of the anterolophid is lower and thinner than that in *C. auster*. The m2 ectomesolophid in *C. dormitor* and *C. aeneus* is quite long and high. In *C. auster*, this ridge is absent or incipient. The m2 entoconid in *C. dormitor* and *C. aeneus* has a smooth and round distobuccal side. The distal arm of the hypoconid is short and does not reach the entoconid. In *C. auster*, the distobuccal side of the entoconid on m2 has a

short ridge or rugose arris. The distal arm of the hypoconid joins this short ridge or is very close to the rugose arris. The posterosinusid of m1–2 in *C. dormitor* and *C. aeneus* is larger than that in *C. auster*. The m3 of *C. dormitor* and *C. aeneus* has bigger and more conical entoconid than that of *C. auster*, as a result the m3 posterosinusid in *C. dormitor* and *C. aeneus* is smaller.

Cricetops minor is represented by a single M1. The two anterocones of this tooth are conical cusps. The connection between them is weak. Only a very low ridge connects the mesial bases of the two cusps. The buccal and lingual spurs of the antherolophule are strong and long, similar to situation in *C. auster*. The hypocone of *C. minor* bears a short mesial arm. This arm connects the mesiolingual base of the metacone. The entoloph, mesoloph and entomesoloph on the M1 of *C. minor* are thin and low, weaker than those in *C. auster*.

Discussion

Maridet and Ni (2013) described a cricetid rodent *Paracricetops virgatoincisus* Maridet & Ni, 2013 discovered from the Lijiawa locality in Yunnan Province, China. *P. virgatoincisus* is much smaller than *C. auster* and other *Cricetops*, but it presents twinned protocone-paracone, hypocone-metacone, protoconid-metaconid and hypoconid–entoconid pairs. Their phylogenetic analysis suggested that *Paracricetops* and *Cricetops* are sister groups. Relatively more plesiomorphic morphology of *Paracricetops* may imply a southern origin of *Paracricetops-Cricetops* clade. Here, a new species of *Cricetops* discovered from the same locality of *Paracricetops* is reported. The discovery presents the first record of *Cricetops* that occurred in the southeastern Asia, and demonstrates that *Paracricetops* and *Cricetops* were indeed contemporaneous and partly sympatric.

If closely related species, such as sister species, have overlapping distribution ranges, such a distribution may be the result of sympatric speciation. Sympatric speciation is usually thought to be less common than allopatric speciation (Bolnick & Fitzpatrick 2007). In the tropic region, however, sympatric speciation may be correlated with the high degree of niche diversification (Tokeshi & Schmid 2002; Forbes et al. 2009). Large area of the tropics provides more opportunities for ecological niche isolation (Terborgh 1973; Rosenzweig 1995), and higher likelihood of sympatric speciation (Gentry 1989; Mittelbach et al. 2007).

The dramatic changes in global climate and sea level during the Eocene–Oligocene transition are associated with the expansion of open habitats, and a major retraction of tropical rainforest to low latitudes (Morley 2000; Zachos et al. 2001; Jaramillo et al. 2006; Licht et al. 2014; Sun et al. 2014). In southern and southeastern Asia, however, mid-latitude areas were connected to the equatorial region by uninterrupted terrestrial habitats (Licht et al. 2014), and tropical rainforests and monsoonal forests still covered a large area during this transitional period (Morley 2011). Li and Ni (2016) and Ni et al. (2016) reported the discoveries of a pen-tailed treeshrew (*Ptilocercus kylin* Li and Ni, 2016) and a diverse primate fauna from the Lijiawa locality. These discoveries suggest that rainforest environments were much more widespread in Asia in early Oligocene than they are today. The tropic forest at Lijiawa locality may have provided enough ecological niche diversification for the origin of *Cricetops* and its sister group *Paracricetops*.

Previously known species of *Cricetops* are common elements in the early Oligocene mammalian faunas from the northern part of Asia. Their bigger body mass compared to other contemporaneous cricetid rodents and more robust cusps with emphasis on transverse wearing were interpreted as adaptation to semi-arid to arid environment (Lindsay 1977). In contrast, *C. auster* and its sister group *Paracricetops* are rare taxa in the Lijiawa mammalian fauna. *Paracricetops* Maridet and Ni, 2013 is larger than *Eucricetodon* Thaler, 1966 and *Eocricetodon* Wang, 2007, but smaller than *C. auster*. *C. auster* from Lijiawa shares similarly large body mass with other *Cricetops*, and are significantly larger than other cricetid or muroid rodents in the Lijiawa mammalian fauna. Their sharp cusps with well-developed crests may suggest a diet (e.g. probably more folivorous diet) different from those *Cricetops* from the northern part of Asia.

Acknowledgement

Disclosure statement

Funding

ORCID

Lüzhou Li http://orcid.org/0000-0002-9453-6900
Xijun Ni http://orcid.org/0000-0002-4328-8695
Xiaoyu Lu http://orcid.org/0000-0003-3701-5217
Qiang Li http://orcid.org/0000-0002-9724-5439

References

Argyropulo AI. 1938. [On the fauna of Tertiary Cricetidae of the USSR]. Compte Rendu (Doklady) de l'Académie des Sciences de l'URSS. 20:223–226.

Bolnick DI, Fitzpatrick BM. 2007. Sympatric speciation: models and empirical evidence. Annu Rev Ecol Evol Syst. 38:459–487.

Carrasco MA, Wahlert JH. 1999. The cranial anatomy of Cricetops dormitor, an Oligocene fossil rodent from Mongolia. Am Mus Novit. 3275:1–14.

Emry RJ, Lucas SG, Tyut'kova LA, Wang B. 1998. The Ergilian-Shandgolian (Eocene–Oligocene) transition in the Zaysan Basin, Kazakstan. Bull Carnegie Mus Nat Hist. 34:298–312.

Erbajeva M, Alexeeva N. 2013. Late Cenozoic mammal faunas of the Baikalian Region: composition, biochronology, dispersal, and correlation with Central Asia. In: Wang X, Flynn LJ, Fortelius M, editors. Fossil mammals of Asia. New York (NY): Columbia University Press; p. 495–507.

Forbes AA, Powell THQ, Stelinski LL, Smith JJ, Feder JL. 2009. Sequential sympatric speciation across trophic levels. Science. 323:776–779.

Gentry AH. 1989. Speciation in tropical forests. In: Holm-Nielsen LB, Nielsen IC, Balslev H, editors. Tropical forests: botanical dynamics, speciation and diversity. San Diego (CA): Academic Press; p. 113–134.

Jaramillo C, Rueda MJ, Mora G. 2006. Cenozoic plant diversity in the neotropics. Science. 311:1893–1896.

Kowalski K. 1974. Middle Oligocene rodents from Mongolia. Palaeontol Pol. 30:148–178.

Li Q, Ni X. 2016. An early Oligocene fossil demonstrates treeshrews are slowly evolving "living fossils". Sci Rep. 6:1–8. doi:http://dx.doi.org/10.1038/srep18627.

Licht A, van Cappelle M, Abels HA, Ladant JB, Trabucho-Alexandre J, France-Lanord C, Donnadieu Y, Vandenberghe J, Rigaudier T, Lécuyer C, et al. 2014. Asian monsoons in a late Eocene greenhouse world. Nature. 513:501–506.

Lindsay EH. 1977. *Simimys* and origin of the cricetidae (Rodentia: Muroidea). Geobios. 10:597–623.

Maridet O, Ni X. 2013. A new cricetid rodent from the early Oligocene of Yunnan, China, and its evolutionary implications for early Eurasian cricetids. J Vert Paleontol. 33:185–194.

Matthew WD, Granger W. 1923. Nine new rodents from the Oligocene of Mongolia. Am Mus Novit. 102:1–10.

Mellett JS. 1968. The Oligocene Hsanda Gol Formation, Mongolia: a revised faunal list. Am Mus Novit. 2318:1–16.

Mittelbach GG, Schemske DW, Cornell HV, Allen AP, Brown JM, Bush MB, Harrison SP, Hurlbert AH, Knowlton N, Lessios HA, et al. 2007. Evolution and the latitudinal diversity gradient: speciation, extinction and biogeography. Ecol Lett. 10:315–331.

Morley RJ. 2000. Origin and evolution of tropical rain forests. New York (NY): Wiley.

Morley RJ. 2011. Cretaceous and tertiary climate change and the past distribution of megathermal rainforests. In: Bush M, Flenley J, Gosling W, editors. Tropical rainforest responses to climatic change. 2nd ed. Berlin: Springer-Verlag; p. 1–34.

Ni X, Flynn JJ, Wyss AR. 2012. Imaging the inner ear in fossil mammals: high-resolution CT scanning and 3-D virtual reconstructions. Palaeontol Electron. 15:1–10.

Ni X, Li Q, Li L, Beard KC. 2016. Oligocene primates from China reveal divergence between African and Asian primate evolution. Science. 352:673–677.

Ni X, Meng J, Wu W, Ye J. 2007. A new Early Oligocene peradectine marsupial (Mammalia) from the Burqin region of Xinjiang, China. Naturwissenschaften. 94:237–241.

Rosenzweig ML. 1995. Species diversity in space and time. Cambridge: Cambridge University Press.

Russell DE, Zhai R. 1987. The Paleogene of Asia: mammals and stratigraphy. Paris: Éditions du Muséum National d'Histoire Naturelle.

Shevyreva NS. 1967. Hamsters of the genus *Cricetodon* from the middle Oligocene of Central Kazakhstan. Paleontol J. 1:78–85.

Sun J, Ni X, Bi S, Wu W, Ye J, Meng J, Windley BF. 2014. Synchronous turnover of flora, fauna, and climate at the Eocene–Oligocene Boundary in Asia. Sci Rep. 4:1–6. doi:http://dx.doi.org/10.1038/srep07463.

Terborgh J. 1973. On the notion of favorableness in plant ecology. Am Nat. 107:481–501.

Tokeshi M, Schmid PE. 2002. Niche division and abundance: an evolutionary perspective. Popul Ecol. 44:189–200.

Wang B. 1985. Zapodidae (Rodentia, Mammalia) from the lower Oligocene of Qujing, Yunnan, China. Mainzer geowiss Mitt. 14:345–367.

Wang B. 1987. Discovery of cricetids (Rodentia, Mammalia) from middle Oligocene of Nei Mongol, China. Vertebr PalAsiatica. 25:187–198.

Wang B. 1992. The Chinese Oligocene: a preliminary review of mammalian localities and local faunas. In: Prothero DR, Berggren WA, editors. Eocene–Oligocene climatic and biotic evolution. Princeton: Princeton University Press; p. 529–547.

Wang B. 1997a. Chronological sequence and subdivision of Chinese Oligocene mammalian faunas. J Stratigr. 21:183–191.

Wang B. 1997b. Problems and recent advances in the division of the continental Oligocene. J Stratigraph. 21:81–90.

Wang B. 2001. Late Eocene Ctenodactyloids (Rodentia, Mammalia) from Qujing, Yunnan, China. Vertebr PalAsiatica. 39:24–42.

Wang B, Chang J, Meng X, Chen J. 1981. Stratigraphy of the Upper and Middle I Oligocene of Qianlishan district, Nei Mongol (Inner Mongolia). Vertebr PalAsiatica. 19:26–34.

Zachos J, Pagani M, Sloan L, Thomas E, Billups K. 2001. Trends, rhythms, and aberrations in global climate 65 Ma to present. Science. 292:686–693.